GIS-based weight-of-evidence modelling of rainfall-induced landslides in small catchments for landslide susceptibility mapping

Ranjan Kumar Dahal . Shuichi Hasegawa . Atsuko Nonomura . Minoru Yamanaka . Takuro Masuda . Katsuhiro Nishino

R. K. Dahal

1 Dept. of Safety Systems Construction Engineering, Faculty of Engineering, Kagawa University, 2217-20, Hayashi-cho, Takamatsu City, 761-0396, Japan

2 Department of Geology, Tri-Chandra Multiple Campus, Tribhuvan University, Ghantaghar, Kathmandu, Nepal

Phone: 0081-87-864-2140

Fax: 0081-87-864-2031

Email: ranjan@ranjan.net.np

URL: http://www.ranjan.net.np

S. Hasegawa . A. Nonomura . M. Yamanaka . T Masuda

Dept. of Safety Systems Construction Engineering, Faculty of Engineering, Kagawa University, 2217-20, Hayashi-ch, Takamatsu City, 761-0396, Japan

K. Nishino

Oyo Corporation, Ichigaya Building, 4-2-6, Kudan North, Chiyoda, Tokyo, 102-0073, Japan

Cite this article as:
Dahal, R.K., Hasegawa, S., Nonomura A., Yamanaka, M., Masuda, T., Nishino K., 2008, GIS-based weights-of-evidence modelling of rainfall-induced landslides in small catchments for landslide susceptibility mapping, Environmental Geology 54 (2): 314-324, DOI: 10.1007/s00254-007-0818-3.

Abstract

Landslide susceptibility mapping is a vital tool for disaster management and planning development activities in mountainous terrains of tropical and subtropical environment. In this paper, the weights-of-evidence modelling was applied, within a geographical information system (GIS), to derive landslide susceptibility map of two small catchments of Shikoku, Japan. The objective of this paper is to evaluate the importance of weights-of-evidence modelling in the generation of landslide susceptibility maps in relatively small catchments having area less than 4 sq km. For study area in Moriyuki and Monnyu catchments, northeast Shikoku Island in west Japan, a dataset was generated at scale 1:5000. Relevant thematic maps representing various factors (e.g. slope, aspect, relief, flow accumulation, soil depth, soil type, landuse and distance to road) that are related to landslide activity were generated using field data and GIS techniques. Both catchments have homogeneous geology and only consist of Cretaceous granitic rock. Thus, bedrock geology was not considered in data layering during GIS analysis. Success rates were also estimated to the evaluate accuracy of landslide susceptibility maps and it is found that the weights-of-evidence modelling is also useful in landslide susceptibility mapping of small catchments.

Introduction

Landslides are amongst the most damaging natural hazards in the mountainous terrain of tropical and subtropical environments. Potential sites that are particularly prone to landslides should therefore be identified in advance so as to reduce disaster damages. Landslide hazard assessment can be a vital tool to understand the basic characteristics of the terrains that are prone to failure especially during extreme climatic events. According to Varnes (1984) the landslide hazard can be assessed in terms of probability of occurrence of a potentially damaging landslide phenomenon within a specified period of time and within a given area. Moreover, intrinsic and extrinsic variables are used to determine landslide hazard in an area (Siddle 1991; Wu and Siddle 1995; Atkinson and Massari 1998; Dai and others 2001; Çevik and Topal, 2003). The intrinsic variables determine the susceptibility of landslides and include bedrock geology, geomorphology, soil depth, soil type, slope gradient, slope aspect, slope convexity and concavity, elevation, engineering properties of the slope material, land use pattern, drainage patterns, and so on. Similarly, the extrinsic variables tend to trigger landslides in an area of given susceptibility, and may include heavy rainfall, earthquakes, and volcanoes. Observations and experiences show that the probability of landslide occurrence depends on both intrinsic and extrinsic variables. However, the extrinsic variables are site specific and possess temporal distribution. Moreover, they are difficult to be estimated because of lack of information about the spatial distribution. Hence, in landslide hazard assessment practice, the term “landslide susceptibility mapping” is addressed without considering the extrinsic variables in determining the probability of occurrence of a landslide event (Dai and others 2001).

Most published literatures on landslide hazard mapping mainly deal with landslide susceptibility mapping. There are numerous studies involving landslide hazard evaluation, and particularly, Guzzetti and others (1999) have summarized many cases of landslide hazard evaluation studies. Landslide susceptibility may also be assessed through heuristic, deterministic, and statistical approaches (Okimura and Kawatani 1986; Yin and Yan 1988; Soeters and Van Westen 1996; Van Westen and Terlien 1996; Gökceoglu and Aksoy, 1996; Pachauri and others 1992; Van Westen 2000; Lee and Min 2001; Dai and others 2001; Zêzere and others 2004; Van Westen and others 2003; Saha and others 2005). Heuristic approach is a direct or semi direct mapping methodology, in which a direct relationship is established between the occurrence of slope failures and the causative terrain parameters during the landslide inventory. Therefore, in this approach, the opinions of the experts are very important to estimate landslide potential from the data involving intrinsic variables. Similarly, assigning weight values and ratings to the variables is very subjective and the results are not reproducible. Deterministic approaches, however, are based on slope stability analyses, and are only applicable when the ground conditions are relatively homogeneous across the study area and the landslide types are known. Mainly, the infinite slope stability model has been widely used to assess landslide susceptibility in deterministic approaches (Wu and Sidle 1995; Terlien 1996; Gökceoglu and Aksoy 1996), and such stability model needs high degree of simplification of the intrinsic variables. Statistical approach, on the other hand, is an indirect susceptibility mapping methodology which involves statistical determination of the

combinations of variables that have led to landslide occurrence in the past. All possible intrinsic variables are entered into a GIS and crossed for their analysis with a landslide inventory map. Both simple or bivariate and multivariate statistical approaches have been used widely in such statistical approach of landslide susceptibility mapping (Siddle and others 1991; Atkinson and Massari 1998; Van Westen 2000; Dai and others 2001).

In the past, the susceptibility assessment and mapping were considered laborious and time consuming jobs, but at present they are comparatively easy due to extreme development in computer applications and geographical information systems (GIS). Keeping this in mind, in this study, the landslide susceptibility was evaluated by GIS technique using the weight-of-evidence modelling with respect to bivariate statistical approach. The study area was selected in north-eastern part of Shikoku Island in west Japan that suffered extensive landslide damage during the heavy typhoon rainfall of 2004 and is a suitable case for the evaluation of the frequency and distribution of rainfall-induced landslides for susceptibility mapping.

The study area

Shikoku is the smallest of the four main islands of Japan (total area: 18,800 km^2), situated south of the island of Honshu and east of the island of Kyushu, between Seto Inland Sea and the Pacific Ocean. It is 225 km long and 50-150 km wide with more than 80% of land consisting of steep mountain slopes. It has few plain areas along the coastal lines and elevated peaks in the central part. The mountains are almost covered by thick forests of subtropical broadleaved trees, Japanese cedars, and Japanese bamboos. The mean annual precipitation of Shikoku ranges from 3,500 to 1,000 mm. Due to the geological and morphological settings, landslides and floods caused by typhoon rainfall are very frequent in Shikoku (Hiura and others 2005; Dahal and others 2006).

Although climate of northern part of Shikoku Island is the inland type climate like Mediterranean region and subsequently have few rainfall (annual rainfall 1000 mm only), the area occasionally suffered by extreme typhoon brought rainfall which sometime exceeds more than 750 mm in one day. In 2004, Shikoku experienced extreme events of typhoon rainfall and faced huge losses of life and property. Kagawa prefecture, the north eastern prefecture of Shikoku, was hit by four typhoons (0415, 0416, 0421, and 0423) in 2004 and suffered loss of lives and property because of the many landslides triggered by typhoon rainfall. Among these disaster events, small river catchments, Moriyuki and Monnyu, situated in eastern part of Kagawa prefecture (Fig. 1), were confronted by hardest hit of typhoon 0423 (Tokage) and suffered by extensive damages. From October 19 through 20, 2004, typhoon 0423 dropped 674 mm and 495 mm of rain in a 48-h period on Moriyuki and Monnyu of eastern Kagawa, respectively. On October 20, a rain-gauge station in the Kusaka pass (located within 1 km aerial distance from Moriyuki catchment) recorded 582 mm of rain in 24-h with maximum 116 mm/h rainfall intensity. Likewise, Monnyu area has rain gauge station close to the failure sites. In this station, on October 20, 412 mm of rain was recorded in 24-h with maximum 76 mm/h rainfall intensity (Fig 2). These are the highest precipitations of those areas in last 30 years. These rainfall events triggered more than 300 landslides in Moriyuki and Monnyu catchment area and debris flows were occurred. Therefore, these two small catchments, Moriyuki and Monnyu, were selected for this study.

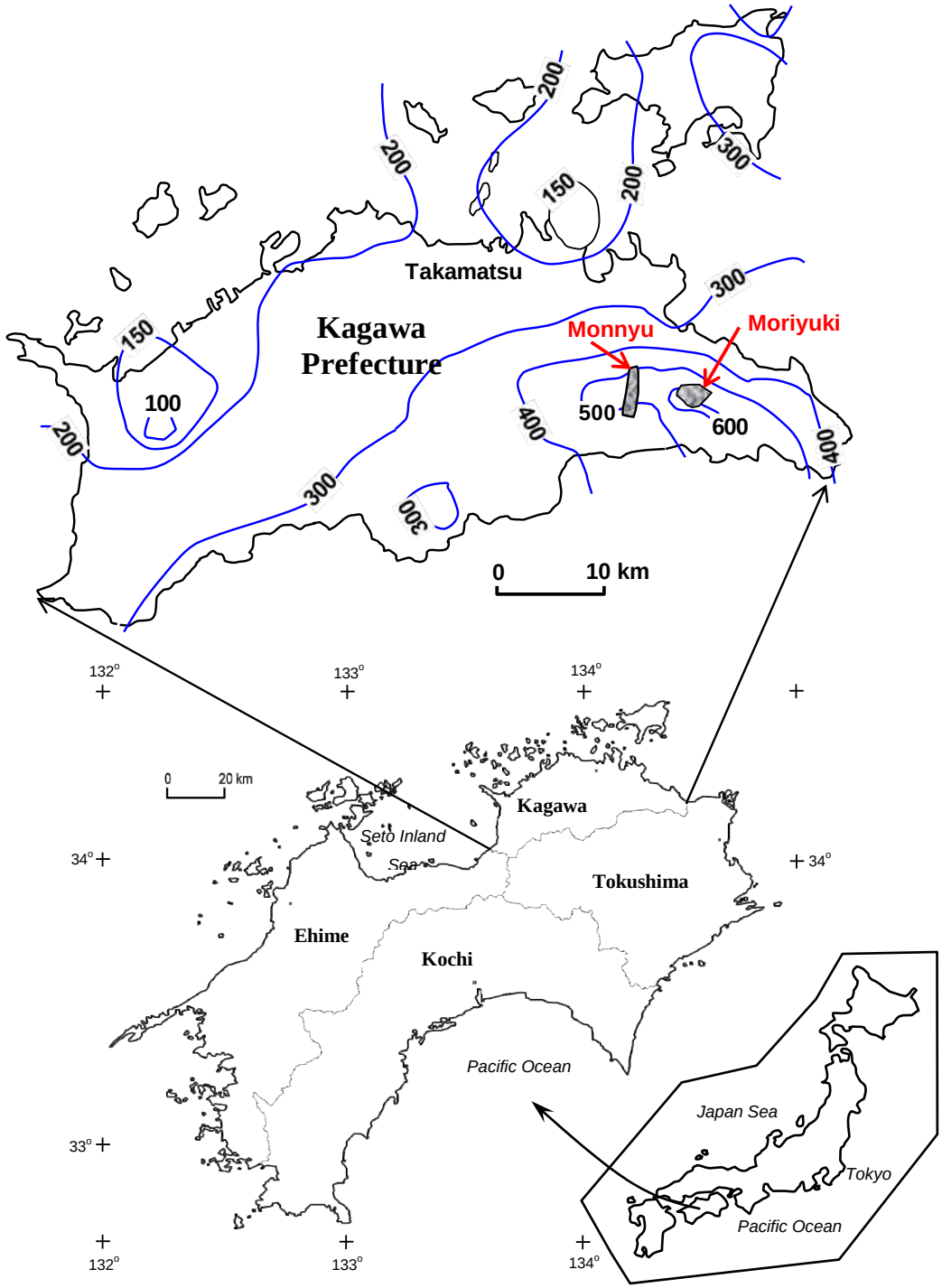

Fig. 1. Location of Moriyuki and Monnyu in north east Shikoku, Japan and rainfall isohyetal map during typhoon 0423 (October 19 and 20, 2004)

Geologically, the study area lies in the Ryoke Belt (Hasegawa and Saito, 1991) of Shikoku. This belt composed of late Cretaceous granitic rocks, late Cretaceous sedimentary rocks (Izumi Group), and Miocene volcanic rocks (Sanuki Group). Particularly, the Moriyuki and Monnyu catchments are situated on zone of Cretaceous granitic rocks (Saito and others 1972).

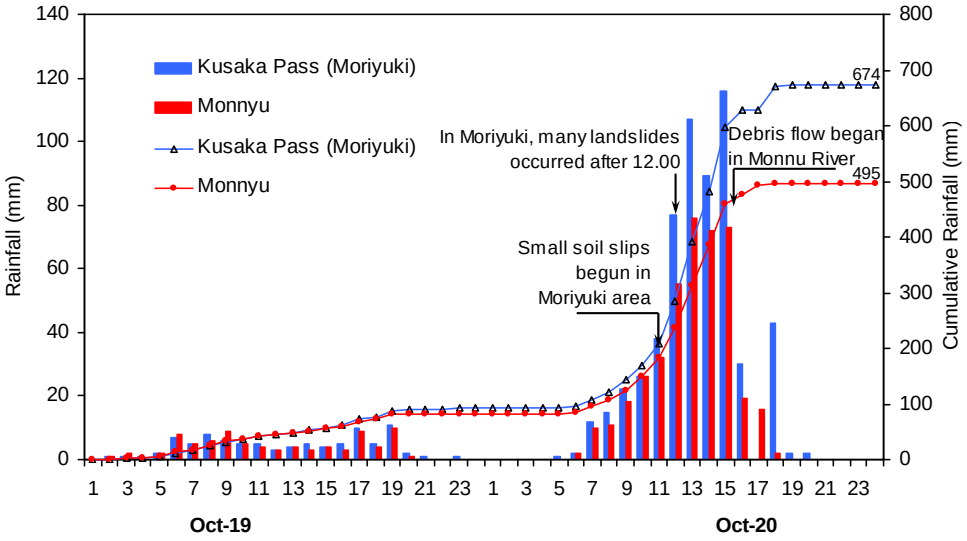

Fig. 2 Rainfall pattern and time of failures in Moriyuki and Monnyu are during typhoon 0423

Weight-of-evidence modelling

In this study, the weight-of-evidence modelling is used for the large scale landslide susceptibility mapping. It uses the Bayesian probability model, and was originally developed for mineral potential assessment (Bonham-Carter and others 1988, 1989; Agterberg and others 1993; Bonham-Carter 1994). Several authors have applied the weight-of-evidence method to mineral potential mapping using the GIS in many countries (Emmanuel and others 2000; Harris and others 2000; Carranza and Hale 2002; Tangestani and Moore 2001). Cheng (2004) used this method for the location of flowing wells and Daneshfar and Benn (2002) used for spatial associations between faults and seismicity. Zahiri and other (2006) used it for mapping of cliff instabilities associated with mine subsidence. This method now also started to apply in landslide susceptibility mapping also (Lee and others 2002; Van Westen and others 2003, Lee and Choi 2004, Lee 2004, Lee and Talib 2005, Lee and Sambath 2006). This method is simple, easy to use and less time consuming (Soeters and Van Westen 1996; Süzen and Doyuran 2004) and it can be performed rather easily with most GIS software packages.

A detailed description of the mathematical formulation of the method is available in Bonham-Carter (1994) and Bonham-Carter et al. (1989). The method calculates the weight for each landslide predictive factor (B) based on the presence or absence of the landslides (L) within the area, as indicated in Bonham-Carter et al. (1994) as follow.

$$W_i^+ = \ln \frac{P\{B|L\}}{P\{B|\bar{L}\}} \quad \ldots\ldots\ldots\ldots\ldots\ldots\ldots\ldots\ldots\ldots \quad (1)$$

$$W_i^- = \ln \frac{P\{\bar{B}|L\}}{P\{\bar{B}|\bar{L}\}} \quad \ldots\ldots\ldots\ldots\ldots\ldots\ldots\ldots\ldots\ldots \quad (2)$$

Where, P is probability and ln is the natural log. Similarly, B is presence of potential landslide predictive factor, $\bar{B}$ is absence of a potential landslide predictive factor, L is presence of landslide, and $\bar{L}$ is absence of a landslide. A positive weight (W_i^+) indicates that the predictable variable is present at the landslide locations and the magnitude of this weight is an

indication of the positive correlation between the presence of the predictable variable and the landslides. A negative weight (W_i^-) indicates the absence of the predictable variable and shows the level of negative correlation. The difference between the two weights is known as the weight contrast, W_f $(W_f = W_i^+ - W_i^-)$; the magnitude of the contrast reflects the overall spatial association between the predictable variable and the landslides.

Although weight-of-evidence modelling has not been previously applied in landslide susceptibility mapping of small catchments, the suitability of the technique for this purpose is evident in its successful use in other studies for examining susceptibility, spatial relationships, and the distribution of particular features. The catchments selected for modelling have typical spatial and physical characters. Both selected catchments have area less than 4 sq km. Both consist of landslides triggered by rainfall and the intrinsic variables are easily quantifiable in field and production of accurate landslide conditioning factor maps is feasible. Two catchments are situated in same climatic condition. Moreover, they have similar bedrock geology, same type of land use pattern, similar engineering properties of soil, and they were affected by same typhoon Tokage in same time and same day. Considering these all typical characters, the main objectives of this study are listed as follows.

- To assess the types of landslides and landslide controlling factors on north eastern terrain of Shikoku Island on a small catchment basis
- To establish weights of intrinsic variables causing landslides in one area (Moriyuki) and apply same methodology for establishing weights of similar type of intrinsic variables in other area (Monnyu)
- To validate of the weight-of-evidence modelling in two catchments having similar intrinsic variables causing landslides triggered by same extrinsic variable (typhoon rainfall)
- To test reliability of weight-of-evidence model for the small catchments those have many similar spatial and physical characters

Data acquisition

For the landslide susceptibility mapping, the main steps were data collection and construction of spatial database from which relevant factors were extracted, followed by assessment of the landslide susceptibility using the relationship between landslide and landslide predictive factors, and validation of results. A key approach of this method is that occurrence possibility of landslide will be comparable with observed landslides.

In initial stage of this study, for each area, a number of thematic data of predictive factors were identified, viz. slope, slope aspect, geology, soil type, soil depth, land use, distance to road etc. Topographic maps, colour aerial photographs taken by Kagawa Prefecture Office immediately after disaster events of 2004 and geological maps of north east Kagawa prepared by Saito and others (1972) were considered as basic data sources to generate these layers. Field surveys were also carried out for data collection and to prepare data layers of various factors as well as to verify geological map prepared by Saito and others (1972). A landslide distribution map was also prepared in field. These data sources were used to generate various

data layers using GIS software ILWIS 3.3. Brief descriptions of each data layer preparation procedure are given here.

1. Landslide characteristics and inventory maps

A landslide inventory map is the simplest output of direct landslide mapping. It shows the location of discernible landslides. It is a key factors used in landslide susceptibility mapping by weight-of-evidence modelling because overlay analysis requires an inventory map. Two hundred and one landslides were detected in Moriyuki catchment and one hundred and forty two landslides were mapped in Monnyu catchment. Landslide inventory maps were prepared in field and later boundary of landslide was again refined by the help of aerial photographs of 1:5000 scale. There were mainly translational and flow types of landslides in both catchments. Both types of failures were mapped out during inventory mapping.

A data sheet was also used to collect information of representative landslides in the study area. Total 76 landslides of Moriyuki and 40 landslides of Monnyu area were visited in field for analysis of nature of slides (length, height, depth, classification etc.) and data sheet was filled for each slide. These landslides were selected on the basis of the following considerations:

- Variations in landslide size, depth, and relative location with respect to slope face and slope morphology (concave, convex and planar) among the total sites.
- Variations in slope orientation, slope height, slope angle, extent of vegetation and thickness of failure.
- Accessibility of slope with respect to investigations and measurements.

From the field study, it was found that the depth of failure was <2 m in more than 70% of slides and more than 70% of slides had length <10 m. Study of volume of failed materials revealed that 95% of landslides had volume less than 1000 m^3, where as in Moriyuki all landslides had volume less than 1000 m^3. Likewise, more than 60% of failure occurred within residual soil and contact of bedrock and residual soil. About 20% of failures were found in fractured bedrocks and few (about 10%) failures were found on contact between bedrock and colluvium and within colluvium.This detail study of selected landslides assists to quantify the overall landslides scenario of the area and also suggests most representative classes for thematic data in GIS analysis.

Landslide inventory maps of both catchments were prepared in GIS, in which, only landslide scars (main failure portion) were used to delineate the landslides. The raster landslide inventory maps of the both area are given in Fig. 3.

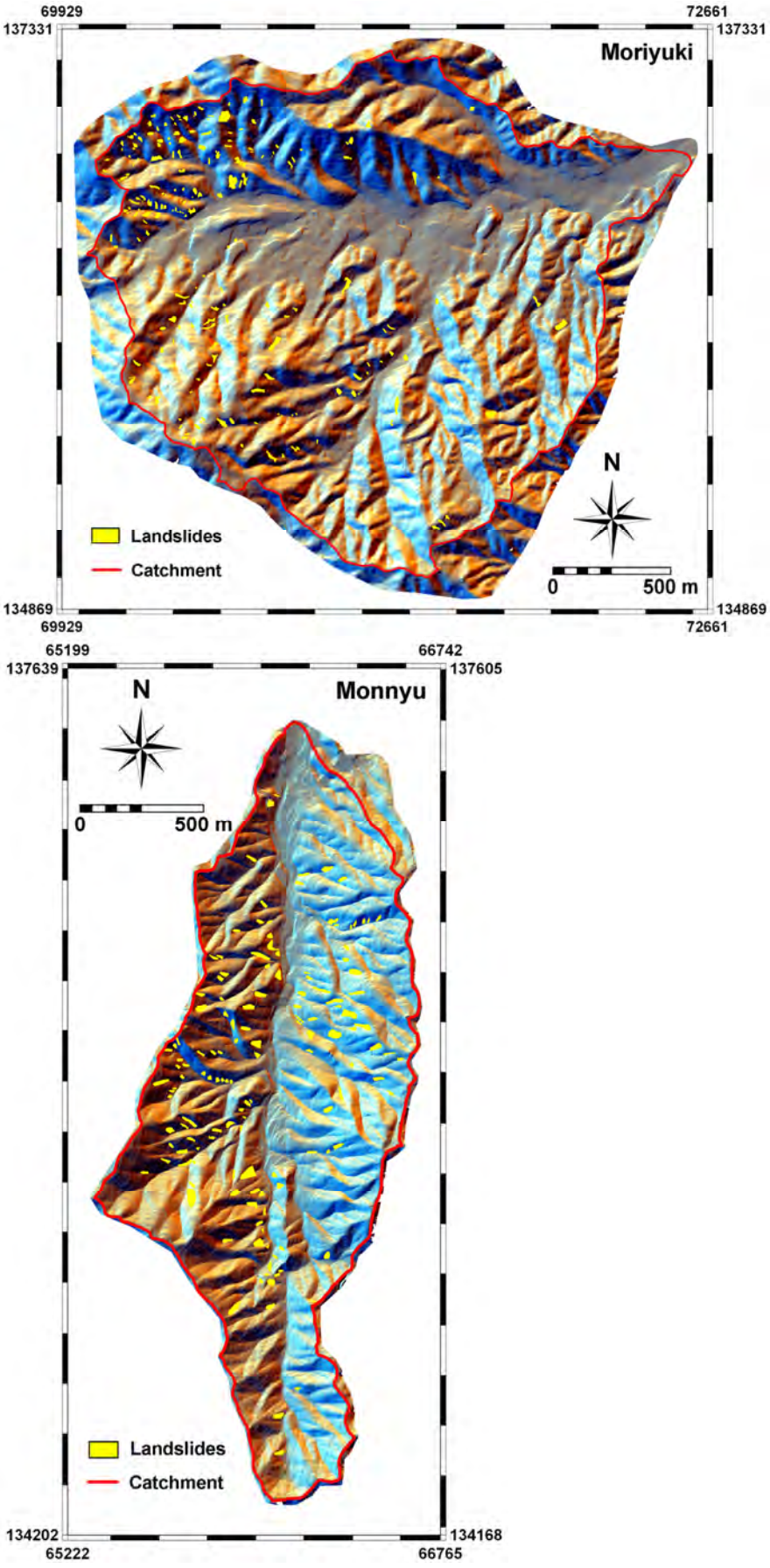

Fig. 3, Landslide inventory map of the Moriyuki and Monnyu catchments

2. Geological maps

Geology plays an important role in landslide susceptibility studies because different geological units have different susceptibilities to active geomorphological processes (Anbalagan 1992; Pachauri and others 1998; Dai and others 2001, Lee and Talib 2005). As mention in earlier section, cretaceous granite is main rock unit of Moriyuki and Monnyu catchments as per the geological map (1:50,000 scale) prepared by Saito and other (1972). During field visit, rock exposures were also investigated specially in terms of mineralogical assemblages. Some thin section slides were also prepared to study minerals under petrological microscope. Mineralogical study confirmed that Cretaceous granitic units in Moriyuki area consist of biotite-granite in northern part whereas southern part has slightly granodioritic affinity. Similarly, In Monnyu, granodiorite is noticed in almost whole area except few area of northern part has little affinity of biotite-granite. Few basaltic veins were also noticed in both catchments. From field study as well as study of existing geological maps and petrological study in lab could not help to identify the spatial distribution of biotite-granite and granodiorite. Thus, it was considered that both catchments have monotonous rock unit and it does not need to consider as potential landslide predictive factor during weight-of-evidence modelling.

3. DEM-based derivatives

A Digital Elevation Model (DEM) representing the terrain is a key to generate various topographic parameters, which influence the landslide activity in an area. Hence, DEM was prepared by digitizing contours of 5 m interval in Moriyuki and 2 m interval in Monnyu from the topographic map of 1:5,000 scale. The digitized contours were interpolated and resampled to 2.5×2.5 m^2 pixel size. From this DEM, thematic data layers like slope, aspect and relative relief have been prepared. Slope data layer, an important parameter in slope stability considerations, comprises of eight classes. This classification was decided after measuring slope angle of failed slope during landslide inventory mapping. Field measurement of total 76 landslides of Moriyuki and 40 landslides of Monnyu catchments signified that most of the landslides occur at slope angle between 26^o to 51^o. Thus, total seven classes, $>10^o$, 10^o-20^o, 20^o-30^o, 30^o-40^o, 40^o-50^o, 50^o-60^o, $>60^o$, were used to prepare slope map. Aspect is referred to as the direction of maximum slope of the terrain surface. For the selected catchments, it is divided into nine classes, namely, N, NE, E, SE, S, SW, W, NW and Flat. Relative relief data layer was prepared from the difference in maximum and minimum elevation and is sliced into eleven classes at 50 m elevation difference.

4. Landuse

Landuse is also one of the key factors responsible for the occurrence of landslides, since, barren slopes are more prone to landslides. In contrast, vegetative areas tend to reduce the action of climatic agents such as rain etc. thereby preventing the erosion due to the natural anchorage provided by the tree roots and, thus, are less prone to landslides (Gray and Leiser 1982; Styczen and Morgan 1995; Greenway 1987). Based on the Aerial photographs taken 10 days after disaster events of 2004 and field visit, nine landuse classes have been considered that may have an impact on landslide activity in the region. These classes are dense forest, sparse forest, shrubs, bare with sparse shrubs, grassland, agriculture, irrigation pond, riverbed,

and settlement. The landuse data layer was generated as vector polygons and they were converted to raster landuse map by employing rasterise operation in ILWIS 3.3.

5. Distance to Road

One of the controlling factors for the stability of slopes is road construction activity. This factor map was generated as per the hypothesis that landslides may be more frequent along roads, due to inappropriate cut slopes and drainage from the road. In order to produce the map showing distance to roads, the road segment map was rasterised and the distance to these roads calculated in meters. The resultant map was then sliced to give a raster map showing distance to roads divided into 7 classes. The seven classes are 0 – 10 m, 10 – 20 m, 20 – 30 m, 30 – 50 m, 50 – 100 m, 100 – 200 m, and >200 m. For both catchments, same classification scheme was used.

6. Flow accumulation

Following rainfall events, water flows from areas of convex curvature and accumulates in areas of concave curvature. This process is known as flow accumulation and usually very remarkable at upstream segment of catchment. Flow accumulation is a measure of the land area that contributes surface water to an area where surface water can accumulate. This parameter was considered as relevant to this study because it defines the locations of water concentration after rainfall and those locations are likely to have a high landslide incidence. Flow accumulation can be explained as the number of pixels, or area, which contributes to runoff of a particular pixel. Flow accumulation measures the area of a watershed that contributes runoff to the pixel. In fact, flow accumulation is also a DEM based derivatives and DEM Hydro-processing operation in ILWIS 3.3 calculates flow accumulation of a watershed. The flow accumulation operation performs a cumulative count of the number of pixels that naturally drain into outlets.

For both, Moriyuki and Monnyu catchments, the flow accumulation maps were prepared and they were classified into 8 classes using histogram information and calculated cumulative percentages. In both catchments, about 50% of area has 3 to 20 cells contributing their flow and main drainage.

7. Soil depth

During field study, detail soil mapping were carried out in order to prepare soil depth map of both catchments. Landslides mapping as per the prescribed data sheet help to categorise most susceptible soil depth in both catchments. From the study of selected landslides, it is noticed that mainly soil depth of 0.5 m to 2 m has maximum susceptibility to failure. There are some failures in zone having 2 to 3.5 m soil depth also. Thus, three soil depth classes: <2 m, 2 to 4 m and >4 m, were established to create thematic layer of soil depth.

8. Soil type

Soils of study area were geologically classified and soil maps were prepared for both catchments. Three categories: alluvial soil, colluvial soil and residual soil deposits were identified in field as per the genesis.

Thus, finally total eight factors maps (slope, aspect, relief, flow accumulation, soil depth, soil type, landuse and distance to road) were selected as thematic data for analysis. The all factor

maps prepared in GIS for both Moriyuki and Monnyu area are given in Fig 4 and Fig 5 respectively. Analysis procedures and results are discussed in following sections.

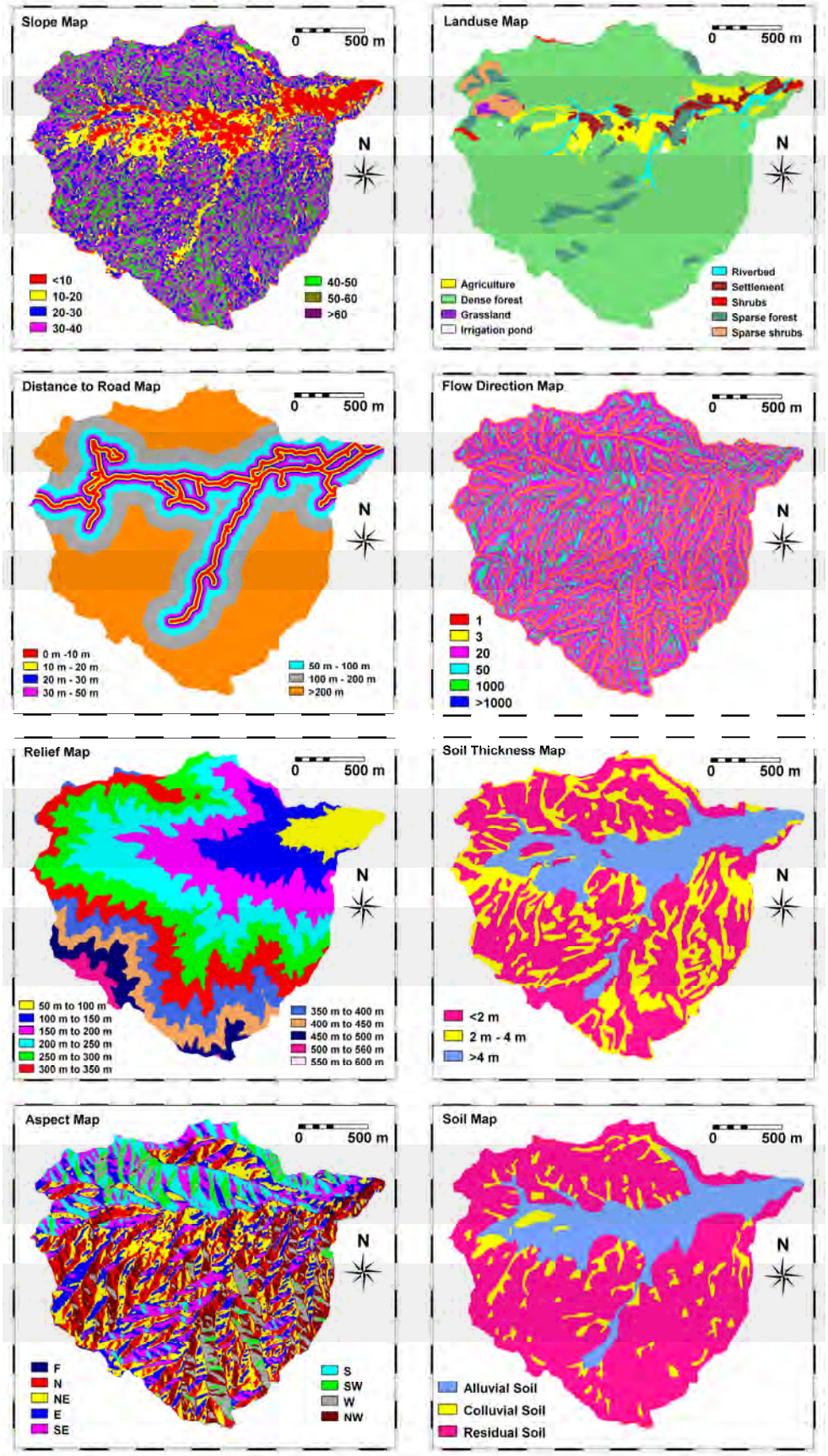

Fig. 4, Various thematic data layers prepared in GIS for Moriyuki area

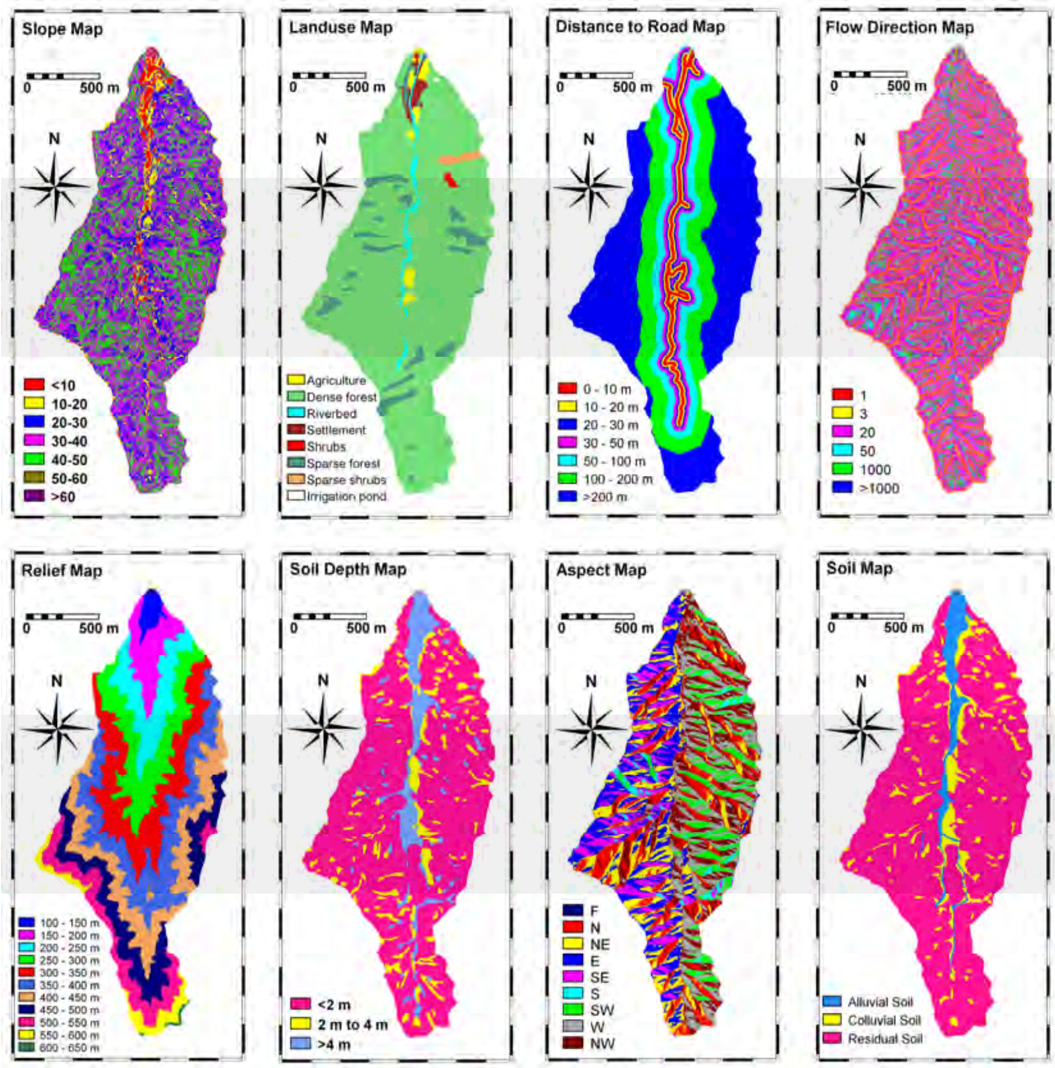

Fig. 5, Various thematic data layers prepared in GIS for Monnyu area

Analysis and Result

To evaluate the contribution of each factor towards landslide hazard, the existing landslide distribution data layer has been compared with various thematic data layers separately. For this purpose, Eq. (1) and (2) were written in number of pixel format as follow.

$$W_i^+ = \ln \frac{\dfrac{Npix_1}{Npix_1 + Npix_2}}{\dfrac{Npix_3}{Npix_3 + Npix_4}} \qquad \text{(3)}$$

$$W_i^- = \ln \frac{\dfrac{Npix_2}{Npix_1 + Npix_2}}{\dfrac{Npix_4}{Npix_3 + Npix_4}} \qquad \text{(4)}$$

Where,

$Npix_1$ is number of pixels representing presence of both potential landslide predictive factor and landslides

$Npix_2$ is number of pixels representing presence of landslides and absence of potential landslide predictive factor

$Npix_3$ is number of pixels representing presence of potential landslide predictive factor and absence of landslides

$Npix_4$ is number of pixels representing absence of both potential landslide predictive factor and landslides

All thematic maps were stored in raster format (985 rows and 1093 columns for Moriyuki catchment and 1390 rows and 628 columns for Monnyu catchment) with a pixel size of 2.5 meters. The factor maps were all combined with the landslide inventory map for the calculation of the positive and negative weights. The calculation procedure was written in the form of a script file in ILWIS 3.3, consisting of a series of GIS command to support Eqs. (3) and (4). Since all of the maps are multi-class maps, containing several classes, the presence of one factor, such as dense forest implies the absence of the other factors of the same landuse map. Therefore in order to obtain the final weight of each factor, the positive weight of the factor itself was added to the negative weight of the other factors in the same map (Van Westen and others 2003). The final calculated weights for both catchments are given in Table 1.

The resulting total weights, as shown in Tables 1, directly indicate the importance of each factor. If the total weight is positive, the factor is favourable for the occurrence of landslides, and if it is negative, it is not. It also can be concluded from Tables 1 that some of the factors show hardly any relation with the occurrence of landslides, as evidenced by weights close to 0. For example, distance from roads classes of both catchments show values that oscillate around zero, without any extreme positive or negative values. This indicates that distance from roads is not a very sensitive predicting factor in both catchments. The frequency ratio (%landslide/%area) assists to assess relationship between the factors and landslide occurrences (Lee and Sambath 2006). For example, slope aspect south-east shows high probability of landslide occurrences in Moriyuki whereas south slope is more vulnerable in Monnyu.

The weights are assigned to the classes of each thematic layers, respectively, to produce weighted thematic maps, which were overlaid and numerically added according to Eq. (5) to produce a Landslide Susceptibility Index (LSI) map.

$$(LSI = W_f Slope + W_f Aspcls + W_f Relief + W_f FA + W_f Soil + W_f Depth + W_f Landuse + W_f Roadis) \quad \text{……..……..... (5)}$$

Where,

$W_f Slope$, $W_f Aspcls$, $W_f Relief$, $W_f FA$, $W_f Soil$, $W_f Depth$, $W_f Landuse$ and $W_f Roadis$ are distribution-derived weight of slope, slope aspect, relief, flow accumulation, soil type, soil depth, landuse, distance to road factor maps, respectively. Thus, two attribute maps of Moriyuki and Monnyu catchments were prepared from respective LSI values. The LSI values are found to lie in the range from -22.820 to 7.224 for Moriyuki and -20.589 to 5.402 for Monnyu.

To check capability of LSI values to predict landslide occurrences were verified by the help of success rate (Chung and Fabbri 1999) curve and effect analysis (Lee 2004, Lee and Talib

2005, Lee and Sambath 2006). The success rate indicates how much percentage of all landslides occurs in the classes with the highest value of susceptibility maps. Effect analysis helps to validate and to check the predictive power of selected factors and classes that are used in susceptibility analysis.

Table 1, Computed weight for classes of various data layers based on landslide occurrences

Name of Catchments	**Moriyuki Catchment**				**Monnyu Catchment**			
Theme Class	Landslides occurences % (total landslide area is 8323 pixels)	Area % (total area of catchment is 563970 pixels)	Ratio (%Landslides/ %Area)	WFINAL	Landslides occurences % (total landslide area is 10511 pixels)	Area % (total area of catchment is 345091 pixels)	Ratio (%Landslides/ %Area)	WFINAL
Slope								
<10	1.54	10.39	0.15	-2.097	0.15	3.49	0.04	-3.223
20-30	4.41	15.95	0.28	-1.506	2.50	8.32	0.30	-1.316
20-30	22.84	24.24	0.94	-0.158	17.38	23.18	0.75	-0.403
30-40	44.76	31.58	1.42	0.493	40.15	38.30	1.05	0.046
40-50	23.21	15.43	1.50	0.436	33.07	23.85	1.39	0.439
50-60	3.09	2.32	1.33	0.222	6.52	2.79	2.33	0.897
>60	0.16	0.09	1.80	0.521	0.23	0.06	3.52	1.309
Slope aspect								
Flat	0.38	3.33	0.12	-2.243	0.00	0.05	0.00	-2.260[a]
North	5.26	15.68	0.34	-0.591	5.60	15.03	0.37	-0.595
North-East	12.58	19.59	0.64	-0.573	7.22	14.36	0.50	-0.799
East	25.75	16.84	1.53	0.507	23.51	17.46	1.35	0.374
South-East	27.20	12.28	2.21	0.962	19.77	8.76	2.26	0.974
South	13.89	8.66	1.60	0.501	8.32	2.41	3.45	1.369
South-West	4.24	4.27	0.99	-0.046	12.82	8.69	1.47	0.438
West	5.03	6.90	0.73	-0.379	14.01	17.63	0.80	-0.293
North-West	5.66	12.46	0.45	-0.914	8.74	15.50	0.56	-0.679
Relief								
50 m to 100 m	0.00	4.84	0.00	-6.779[a]	-	-	-	-
100 m to 150 m	0.26	9.65	0.03	-3.762	0.06	1.76	0.03	-3.515
150 m to 200 m	6.69	14.08	0.48	-0.885	2.69	5.95	0.45	-0.885
200 m to 250 m	19.10	18.42	1.04	-0.004	11.25	8.91	1.26	0.226
250 m to 300 m	30.94	17.71	1.75	0.697	13.10	12.35	1.06	0.027
300 m to 350 m	23.31	13.76	1.69	0.607	24.02	15.66	1.53	0.509
350 m to 400 m	5.41	8.79	0.61	-0.579	27.13	16.94	1.60	0.582
400 m to 450 m	4.35	6.65	0.65	-0.504	14.02	14.82	0.95	-0.109
450 m to 500 m	6.84	4.56	1.50	0.388	6.71	11.54	0.58	-0.653
500 m to 550 m	2.60	1.43	1.81	0.569	1.01	8.43	0.12	-2.272
550 m to 600 m	0.50	0.11	4.47	1.505	0.00	3.37	0.00	-6.453[a]
600 m to 650 m	-	-	-	-	0.00	0.28	0.00	-3.931[a]
Flow Accumulation								
1	6.27	10.48	0.60	-0.636	9.12	14.00	0.65	-0.501
3	10.79	17.10	0.63	-0.610	11.94	18.91	0.63	-0.565
20	60.17	54.56	1.10	0.163	51.39	49.82	1.03	0.055
50	15.11	10.91	1.39	0.311	15.74	10.26	1.53	0.499
1000	6.88	5.16	1.33	0.242	10.15	5.18	1.96	0.749
>1000	0.77	1.79	0.43	-0.933	1.66	1.83	0.90	-0.115
Soil Type								
Alluvial Soil	1.75	18.98	0.09	-3.095	0.50	6.07	0.08	-3.539
Colluvial Soil	13.01	9.36	1.39	-0.128	5.29	10.69	0.50	-1.742
Residual Soil	85.23	71.66	1.19	0.330	94.21	83.25	1.13	0.248
Soil Depth								
<2 m	76.17	53.66	1.42	0.626	96.41	78.35	1.23	0.414
2 m to 4 m	21.49	27.88	0.77	-0.753	1.10	10.63	0.10	-4.021
>4 m	2.33	18.45	0.13	-2.668	2.48	11.02	0.23	-3.234
Landuse								
Agriculture	0.19	5.55	0.03	-3.037	0.00	1.62	0.00	-5.391[a]
Dense forest	68.59	81.60	0.84	-0.326	78.78	87.01	0.91	-0.204
Grassland	3.30	0.25	13.09	3.199	0.00	0.04	0.00	-0.999a
Irrigation pond	0.00	0.12	0.00	-1.895[a]	-	-	-	-
Riverbed	0.00	1.87	0.00	-4.687[a]	0.20	1.84	0.11	-1.620[a]
Settlement	0.00	2.68	0.00	-5.055[a]	0.53	1.11	0.48	-0.345
Shrubs	0.67	0.40	1.69	0.931	0.90	0.26	3.54	1.770
Sparse forest	15.44	5.63	2.74	1.541	17.60	7.24	2.43	1.472
Sparse shrubs	11.80	1.90	6.22	2.412	1.98	0.78	2.53	1.407
Distance to Roads								
0 m - 10 m	2.82	5.18	0.55	-0.615	2.69	4.17	0.65	-0.438
10 m - 20 m	4.23	4.34	0.97	-0.004	3.39	3.54	0.96	-0.021
20 m - 30 m	3.65	3.83	0.95	-0.028	4.61	3.24	1.43	0.411
30 m - 50 m	4.97	6.57	0.76	-0.277	9.11	5.63	1.62	0.569
50 m - 100 m	13.72	13.04	1.05	0.082	14.21	13.07	1.09	0.128
100 m - 200 m	31.88	19.95	1.60	0.664	23.31	23.91	0.97	-0.006
>200 m	38.72	47.08	0.82	-0.324	42.67	46.44	0.92	-0.128

[a] In this value landslide occurrence is 0, so arbitary 1 pixel was consider during calculation of WFinal

Three landslide susceptibility index maps were prepared for each area and named as Main, Case A and Case B landslide susceptibility maps. Main map prepared by adding all weight as per the Eq. 5. Case A susceptibility map was prepared by adding W_fSlope, W_fFA, W_fSoil, and W_fDepth whereas Case B map was prepared by adding W_fSlope, W_fFA, W_fSoil, W_fDepth, W_fRelief and W_fLanduse. The success rate curve of all three maps of both Moriyuki and Monnyu are shown in Fig 6. These curves explain how well the model and factors predict landslides. To obtain the success rate curve for each LSI map, the calculated index values of all pixels in maps were sorted in descending order. Then the ordered pixel values were categorised into 100 classes with 1% cumulative intervals. These classified maps were crossed with landslide inventory map. Then the success rate curve was made from cross table value. In the case of Moriyuki, when all factor was used (Main map), 10% class of the study area where the LSI had a higher rank and could explain 46% of all landslides. Likewise, 30% of LSI value could explain 72% of all landslides. Similarly, in the case of Monnyu area, 15% of area where the LSI had a higher rank could explain 50% of all landslides. Fig 6 provides percentage coverage of landslides in various higher rank percentage of LSI. By the help of this success rate curve of Main map of Moriyuki, corresponding value of LSI in 10%, 30%, 50% and 70% class were selected and five landslide susceptibility zones, viz. very low, low, moderate, high and very high were established to prepare the classified landslide susceptibility maps after weight-of-evidence modelling (Fig 7). Similar procedure were used for Monnyu area also but corresponding value of LSI in 15%, 35%, 55% and 75% class were selected as per the concentration of landslide percentage. The susceptibility map of Monnyu area after weight-of-evidence modelling is given in Fig 8.

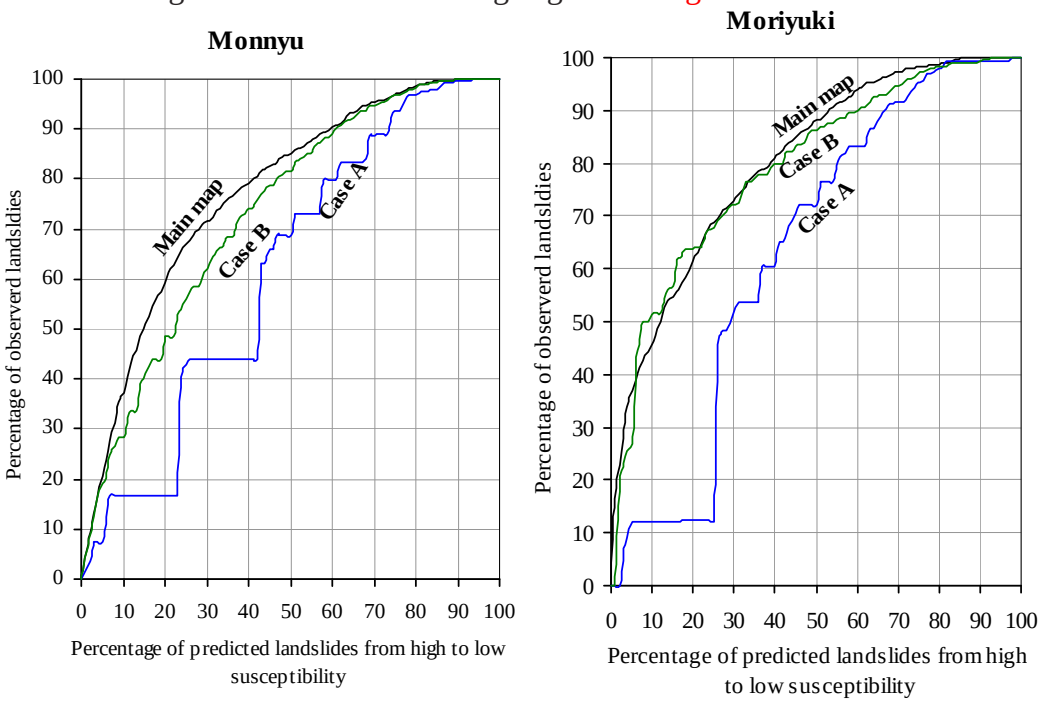

Fig. 6, Success rate curves of main susceptibility maps of Moriyuki and Monnyu and other two cases, details are given in text

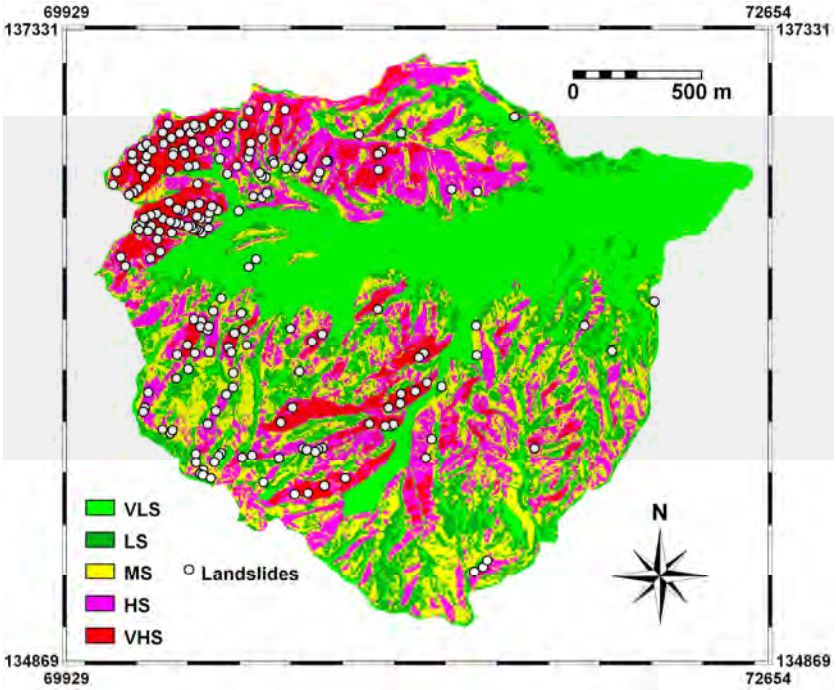

Fig. 7, Landslide susceptibility map of Moriyuki catchment, VHS: very high susceptibility, HS: high susceptibility, MS: moderate susceptibility, LS: low susceptibility, VLS: very low susceptibility

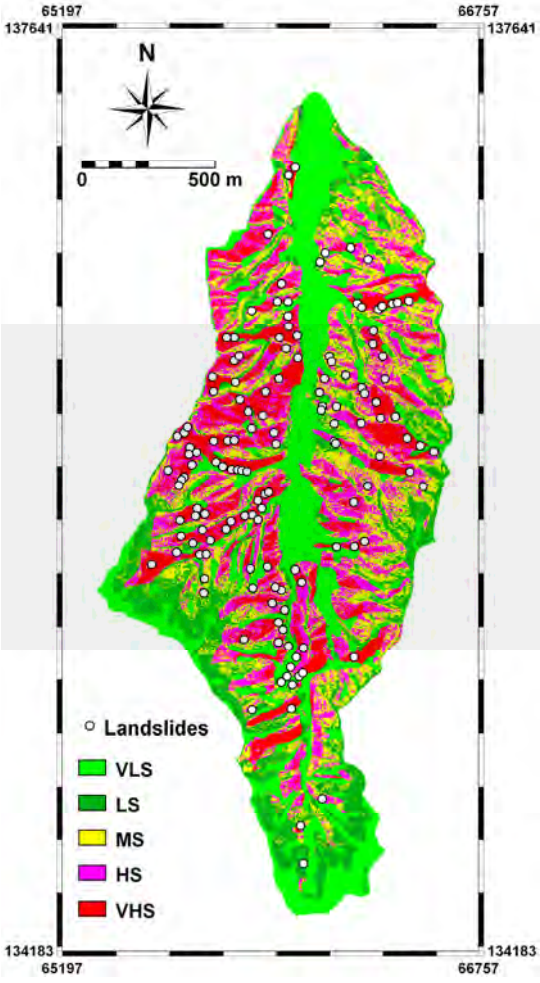

Fig. 8, Landslide susceptibility map of Monnyu catchment, VHS: very high susceptibility, HS: high susceptibility, MS: moderate susceptibility, LS: low susceptibility, VLS: very low susceptibility

To compare the landslide susceptibility results, area under the curves (Lee 2004, Lee and Talib 2005, Lee 2005, Lee and Sambath 2006) were estimated from the rate graphs (see Fig 6). A total area equal to one denotes perfect prediction accuracy for all three cases. This area under the curve qualitatively measures the prediction accuracy of LSI value. In both catchments, it is realized that susceptibility map prepared as per Case A is worst case and main map prepared after joining all available predicting factor as per Eq. 5 is the best one. The verification demonstrates (Fig 6 and Table 2) that main map of both catchments show high value of area under the curve in comparison to Case A and Case B. The area under the curve of Moriyuki catchment shows maximum 80.7% accuracy of prediction whereas same of Monnyu catchment shows 77.6% accuracy. Similarly, area under the curve of Case B of both catchments illustrates that the selected factor parameters slope aspect and distance to roads have less effect in this weight-of-evidence modelling because significant increment of prediction rate could not noticed after adding their value in the modelling (Table 2). The success rate curves of Case A of both catchments explain variable distribution of prediction. Thus, from the qualitative study of area under the curve of success rates, it is realized that main maps of both catchments showed satisfactory agreement between the susceptibility map and landslides location data.

Table 2, Area under the curve after weight-of-evidence modelling

Catchments		**Main map**	**Case A**	**Case B**
Moriyuki	Area below the curve	8066	6395	7972
	Ratio of the area	0.807	0.639	0.797
Monnyu	Area below the curve	7757	6192	7367
	Ratio of the area	0.776	0.619	0.737

Conclusions

Landslide cause enormous loss of life and property every year in mountainous area. In such area, landslide susceptibility mapping is very essential to delineate landslide prone area. Various methodologies have been proposed for landslide susceptibility mappings, but in this study, weight-of-evidence modelling with respect to bivariate statistical methods was used because data acquisition and analysis is relatively easy and less time consuming. The modelling is applied in two small catchments by considering eight predictive factors. The thematic layers of all predictive factors and existing landslides were prepared in GIS (ILWIS 3.3). Mainly DEM-based derivates and field data are used to prepare data layers of predictive factors. The selected both study areas have typical similarity in geology, soil, relief and landuse. In both catchments, typhoon rainfall was the main triggering factor of landslides. As this study is only dealing with landslide susceptibility and not landslide hazard, information on triggering factors rainfall was not taken into account in this modelling. From this study, following conclusions were made.

- Similar approach of weight-of-evidence modelling able to predict nearly 80% of all landslides in both catchments. This concludes that weight-of-evidence modelling can be also useful in relatively small catchments.
- In many approach of modelling in GIS, model is always employed in only one area. The approach used in that model when employ in other area, there is very few chance of

success. This usually happen because there is lack of similarity of intrinsic variables in the selected sites. But, in this study, landslide susceptibility mapping in two catchments of different area shows analogous and high success rate because of similarity in intrinsic variables and classes. This is the reliability test of weight-of-evidence modelling in small catchments and results are very promising.

- This study also concludes that the approach of GIS-based modelling can give good results in analysis of field oriented data.
- Moreover, planning of any project in local level requires large scale and more accurate landslide susceptibility mapping. The attempt made in this study address that need in some extent. Landslide susceptibility mapping in small catchment scale covers many information that is necessary for local level planner.

Acknowledgments

We thank Mr. Toshiaki Nishimura and Mr. Eitaro Masuda for their help in the field data collection. We also acknowledge Kagawa Prefecture Office and Ministry of Local Development Kagawa for providing aerial photographs and data. Thanks are due to Mr. Birendra Piya, senior geologist, Department of Mines and Geology, Government of Nepal, Kathmandu for his technical assistance and comments. We would also like to thank Dr. Netra Prakash Bhandary, Ehime University, Japan for his comments on the original manuscript. Mr. Anjan Kumar Dahal and Ms. Seiko Tsuruta are sincerely acknowledged for their technical support during the preparation of this paper.

References

Agterberg FP, Bonham-Carter GF, Cheng Q, Wright DF (1993) Weights of evidence modeling and weighted logistic regression for mineral potential mapping. In: Davis JC, Herzfeld UC (eds) Computers in geology, 25 years of progress. Oxford University Press, Oxford, pp 13–32

Anbalagan D (1992) Landslide hazard evaluation and zonation mapping in mountainous terrain. Eng Geol 32: 269–277

Atkinson PM, Massari R (1998) Generalized linear modelling of landslide susceptibility in the Central Apennines, Italy. Comput Geosci 24(4):373–385

Bonham-Carter GF, Agterberg FP, Wright DF (1988) Integration of geological datasets for gold exploration in Nova Scotia. Photogram Eng Remo Sens 54:1585–1592

Bonham-Carter GF, Agterberg FP, Wright DF (1989) Weights of evidence modelling: a new approach to mapping mineral potential. Stat Appl Earth Sci Geol Survey Can Paper 89–9:171–183

Bonham-Carter, GF (1994), Geographic Information Systems for Geoscientists; modelling with GIS, Comp. Meth. Geos., Vol. 13, Pergamon Press, pp. 398.

Carranza EJM, Hale M (2002) Spatial association of mineral occurrences and curvilinear geological features. Math Geol 34:203–221

Çevik E, Topal T (2003) GIS-based landslide susceptibility mapping for a problematic segment of the natural gas pipeline, Hendek (Turkey), Environmental Geology 44:949–962

Cheng Q (2004) Application of weights of evidence method for assessment of flowing wells in the Greater Toronto area, Canada. Nat Resour Res 13:77–86

Chung CF and Fabbri AG (1999) Probabilistic prediction models for landslide hazard mapping, Photogrammetric Engineering & Remote Sensing 65(12), 1389–1399

Dahal RK, Hasegawa S, Yamanaka M and Nishino K (2006) Rainfall triggered flow-like landslides: understanding from southern hills of Kathmandu, Nepal and northern Shikoku, Japan. Proc 10th Int Congr of IAEG, The Geological Society of London, IAEG2006 Paper number 819 :1-14 (CD-ROM)

Dai FC, Lee CF, Li J, Xu ZW (2001) Assessment of landslide susceptibility on the natural terrain of Lantau Island, Hong Kong. Environ Geol 40:381–391

Daneshfar B, Benn K (2002) Spatial relationships between natural seismicity and faults, southeastern Ontario and north-central New York state. Tectonophysics 353:31–44

Emmanuel J, Carranza M, Martin Hale (2000) Geologically constrained probabilistic mapping of gold potential, Baguio district, Philippines. Nat Resour Res 9:237–253

Gökceoglu C, Aksoy H (1999) Landslide susceptibility mapping of the slopes in the residual soils of the Mengen region (Turkey) by deterministic stability analyses and image processing techniques, Engineering Geology 44, pp 147-161

Gray DH, Leiser AT (1982) Biotechnical slope protection and erosion control. Van Nostrand Reinhold, New York

Greenway DR (1987) Vegetation and slope stability. In: Anderson MG, Richards KS (eds) Slope stability. Wiley, New York, pp 187–230

Guzetti F, Carrara A, Cardinali M, Reichenbach P (1999) Landslide hazard evaluation: a review of current techniques and their application in a multi-scale study, central Italy. Geomorphology 31: 181–216

Harris JR, Wilkinson L, Grunsky EC (2000) Effective use and interpretation of lithogeochemical data in regional mineral exploration programs: application of geographic information systems (GIS) technology. Ore Geol Rev 16:107–143

Hasegawa S and Saito M (1991) Natural Environment, Topography and Geology of Shikoku, Tsushi-to-Kiso, Japanese Geotechnical Society, Vol. 39-9 (404): 19-24 (In Japanese)

Hiura H, Kaibori M, Suemine A, Yokoyama S and Murai M, (2005) Sediment related disasters generated by Typhoons in 2004, In Senneset, K., Flaate, K. and Larsen, J.O., ed., Landslides and avalanches ICFL2005 Norway, pp 157-163

Lee S, Choi J (2004) Landslide susceptibility mapping using GIS and the weight-of-evidence model. Int J Geo gr Inf Sci 18:789–814

Lee S, Choi J, Min K (2002) Landslide susceptibility analysis and verification using the Bayesian probability model. Environ Geol 43:120–131

Lee S, Min K (2001) Statistical analysis of landslide susceptibility at Yongin, Korea. Environ Geol 40:1095–1113

Lee S (2004) Application of likelihood Ratio and Logistic Regression Models to Landslide Susceptibility mapping in GIS, Environemtnal Management Vol 34(2):223-232

Lee S and Talib JA (2005) Probabilistic landslide susceptibility and factor effect analysis, Environ Geol 47: 982-990

Lee S (2005) Application of logistic regression model and its validation for landslide susceptibility mapping using GIS and remote sensing data, International Journal of Remote Sensing, Vol. 26 (7): 1477-1491.

Lee S, Sambath T (2006) Landslide susceptibility mapping in the Damrei Romel area, Cambodia using frequency ratio and logistic regression models, Environ Geol 50:847-855

Okimura T, Kawatani T (1986) Mapping of the potential surface-failure sites on granite mountain slopes. In: Gardiner V (ed) Int Geomorp Part I. Wiley, New York, pp 121–138

Pachauri AK, Gupta PV, Chander R (1998) Landslide zoning in a part of the Garhwal Himalayas. Environ Geol 36:325–334

Saha AK, Gupta RP, Sarkar I, Arora MK, Csaplovics E (2005) An approach for GIS-based statistical landslide susceptibility zonation - with a case study in the Himalayas, Landslides 2:61-69

Saito M, Yuuji B, Mitsunobu F, 1972, Subsurface geological map of Sanbonmatsu, north east Kagawa (scale 1:50,000), published by Economic Planning Agency, Kagawa Prefecture Ofiice

Siddle HJ, Jones DB, and Payne HR 1991. Development of a methodology for landslip potential mapping in the Rhondda Valley In: Chandler, R.J. (ed.) Slope Stability Engineering. London: Thomas Telford. pp 137-142.

Soeters, R. and Van Westen C. J.: 1996, Slope Instability Recognition, Analysis and Zonation, In:

Styczen, M.E. and Morgan, R.P.C. 1995, 'Engineering properties of vegetation', in R.P.C. Morgan & R.J. Rickson (eds), Slope Stabilisation and Erosion Control: a bioengineering approach, E&FN Spon, London, pp 5-58.

Süzen ML, Doyuran V (2004), A comparison of the GIS based landslide susceptibility assessment methods: multivariate versus bivariate, Environmental Geology (2004) 45:665-679.

Tangestani MH, Moore F (2001) Porphyry copper potential mapping using the weights-of-evidence model in a GIS, northern Shahr-e-Babak, Iran. Aust J Earth Sci 48:695–701

Terlien, M. T. J.: 1996, Modelling spatial and temporal variations in rainfall-triggered landslides, PhD thesis, ITC Publ. Nr. 32, Enschede, The Netherlands, 254 pp.

Turner, A. K. and Schuster, R. L. (eds), Landslides, investigation and mitigation, Transportation Research Board, National Research Council, Special Report 247, National Academy Press, Washington D.C., U.S.A. pp 129–177.

Van Westen CJ (2000) The modelling of landslide hazards using GIS, Survey in Geophysics 21:241-255

Van Westen CJ, Bonilla JBA (1990) Mountain hazard analysis using a PC-based GIS. In: Price DG (ed) Proc 6th Int Congr of IAEG, AA Balkema, Rotterdam, Publ 1: 265–271

Van Westen CJ, Rengers N, Soeters R (2003) Use of geomorphological information in indirect landslide susceptibility assessment, Natural Hazards 30: 399-419

Van Westen CJ, Rengers N, Terlien MTJ, Soeters R (1997) Prediction of the occurrence of slope instability phenomena through GIS-based hazard zonation. Geol Rundsch 86: 404–414

Van Westen CJ, Terlien TJ (1996) An approach towards deterministic landslide hazard analysis in GIS. A case study from Manizales (Colombia). Earth Surf Proc Landforms 21:853–868

Varnes, D. J.: 1984, Landslide Hazard Zonation: a review of principles and practice, Commission on landslides of the IAEG, UNESCO, Natural Hazards No. 3, 61 pp.

Wu W, Siddle RC (1995) A distributed slope stability model for steep forested basins. Water Resour Res 31:2097–2110

Yin KL, Yan TZ (1988) Statistical prediction model for slope instability of metamorphosed rocks. In: Proceedings of 5th Int Symp on Landslides, Lausanne, Switzerland 2:1269–1272

Zahiri H, Palamara DR, Flentje P, Brassington GM, Baafi E (2006) A GIS-based Weights-of-Evidence model for mapping cliff instabilities associated with mine subsidence, Environ Geol 51: 377–386

Zêzere JL, Rodrigues ML, Reis E, Garcia R, Oliveira S, Vieira G, Ferreira AB (2004) Spatial and temporal data management for the probabilitic landslide hazard assessment considering landslide typology, In Landslides: Evaluation and Stabilization, Lacerda, Ehrlich, Fontoura and Sayâo (eds), Taylor & Fancis Group, London, V 1: 117-123